DRUG ANALYTICAL RESEARCH
ISSN: 2527-2616 *www.seer.ufrgs.br/dar*

Simultaneous assessment of nitrosamines NDBA, NDEA, NDMA, and NDIPA: quantitative and qualitative analysis using FTMIR KBr pellets and ATR-FTMIR spectroscopy

Paulo Roberto Rodrigues Martini *[a], Elton Luís Gasparotto Denardin [b], Clésio Soldateli Paim [b], Andreas Sebastian Loureiro Mendez [a]

[a]*Programa de Pós-Graduação em Ciências Farmacêuticas, Universidade Federal do Rio Grande do Sul (UFRGS), Porto Alegre-RS, Brazil;*
[b]*Programa de Pós-Graduação em Ciências Farmacêuticas, Fundação Universidade Federal do Pampa (UNIPAMPA), Uruguaiana-RS, Brazil.*
**Corresponding author: paulomartini@unipampa.edu.br*

Since nitrosamines (NAs) were first detected in pharmaceutical products in July 2018, new quality assurance and quality control (QA/QC) strategies have emerged. However, few studies have explored the use of conventional FTMIR or ATR-FTMIR spectroscopy for quantifying these impurities. This study evaluated and compared the analytical performance of both ATR-FTMIR and FTMIR KBr-pellet methods for the quantification of four nitrosamines: NDMA, NDEA, NDIPA, and NDBA. Limits of detection (LOD) and quantification (LOQ) were determined for each compound using both techniques. Initially, NDEA was analyzed in methanol solution; subsequently, all four nitrosamines were assessed in potassium bromide (KBr) matrices using both methodologies simultaneously. For NDEA in methanol, the ATR-FTMIR method yielded an LOD of 2.77×10^{-3}% (v/v) and an LOQ of 9.22×10^{-3}% (v/v). For NDMA analyzed by ATR-FTMIR with KBr, the LOD and LOQ were approximately 4.94×10^{-4}% and 1.65×10^{-3}%, respectively. The best sensitivity was achieved for NDBA using the FTMIR KBr-pellet method, which gave the lowest overall values: an LOD of 5.52×10^{-6}% and an LOQ of 1.83×10^{-5}%. The four nitrosamines exhibited distinct physicochemical properties that influenced their spectral responses and, consequently, their analytical performance under the tested conditions. When comparing the two techniques, only the FTMIR KBr-pellet method yielded LODs within regulatory limits for the qualitative detection of NDBA and NDIPA, indicating its superior sensitivity for these compounds.

Keywords: Nitrosamines; FTMIR; ATR; LOQ; LOD

Article received at 03/26/2026 and accepted at 06/27/2026.
https://doi.org/10.22456/dar.v10i1.154434

Introduction

Before June 2018, nitrosamines (NAs) were not listed among the organic impurities in pharmacopeial methods or guidelines by Regulatory Authorities. Consequently, they were not routinely evaluated in active pharmaceutical ingredients (APIs) or finished pharmaceutical products (1).

However, in July 2018, the European Medicines Agency (EMA) became the first to announce a recall of Angiotensin II receptor blockers (ARBs)-based products, also known "sartans" across all European countries, specifically valsartan due to the detection of concerning amounts of NDMA (2). Since the 1950s, NAs have been recognized as strong genotoxic compounds known for their mutagenic and carcinogenic effects in many animal species (3,4).

The NAs N-nitrosodimethylamine (NDMA) and N-nitrosodiethylamine (NDEA) have been classified as probable human carcinogens (Group 2A), and N-nitroso-di-n-propylamine (NDPA), N-nitrosomethylethylamine (NMEA), N-nitrosomorpholine (NMOR), N-nitrosopyrrolidine (NPYR), N-nitrosopiperidine (NPIP), and N-nitroso-di-nbutylamine (NDBA) as possible human carcinogens (Group 2B). Other nitrosamines such as N-nitrosodiisopropylamine (NDIPA), N-nitrosoethylisopropylamine (NEIPA), and N-nitroso-N-methyl-4-aminobutyric acid (NMBA) have been subsequently found in various medications and sartan-based products (Figure 1) (5) Spectroscopic technologies and spectrophotometry procedures are the most popular and attractive analytical approaches due to their simplicity and lower cost compared to other analytical techniques (6). In this context, the infrared spectroscopy is a powerful analytical tool, widely employed in fundamental sciences (7).

Vibrational spectroscopy encompasses several analytical techniques, including mid-infrared (MIR), near-infrared (NIR), and Regional Atmospheric Measurement and Analysis Network (Raman) spectroscopy. The application of these techniques has grown considerably due to their low operational cost, rapid analysis, non-destructive nature, minimal sample consumption, and reduced or even eliminated need for chemical reagents. Furthermore, when attenuated total reflectance (ATR) is employed, sample preparation is often unnecessary, simplifying the analytical workflow and enabling operation by

non-specialized personnel. These advantages, combined with their high accuracy, reliability, and robustness, make vibrational spectroscopic methods attractive alternatives to conventional analytical techniques (8,9).

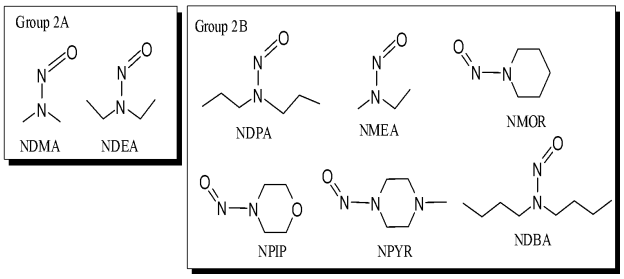

Figure 1. Chemical structures of NAs classified as Group 2A and Group 2B.

The combination of MIR spectroscopy (4000-400 cm^{-1}) with Fourier transform (FTMIR) constitutes one of the most advanced forms of vibrational spectroscopy. Current FTMIR equipment employs an approach that allows for the rapid acquisition of multiple spectra from the same sample. This process reduces the signal-to-noise (S/N) ratio through spectral addition and the application of corresponding transform algorithms, enhancing the accuracy and reliability of the analysis (10). FTMIR using KBr pellet or disk support is a classical infrared spectroscopy technique used to evaluate organic chemicals. The sample is finely ground and intimately mixed with the ground alkali halide at a concentration of 0.5–1 wt% (0.5–1 mg per 100 mg), typically using a mortar and pestle made of agate. The powder mixture is then pressed (10 ton approximately by 5 minutes) into a transparent disk or pellet using an appropriate press (11).
Attenuated Total Reflectance Fourier Transform Mid-Infrared Spectroscopy (ATR-FTMIR) has emerged as a powerful, versatile tool for infrared sampling (12).
ATR methodology is based on direct interaction between a sample and a high-refractive index crystal, usually ZnSe, Ge, Si, or diamond, without the use of KBr. The system creates evanescent waves that enter the sample and detect variations in an internally reflected infrared beam to produce a spectrum (13). ATR-FTMIR spectroscopy particularly, offers several advantages over other methods, including being faster, non-destructive, cost-effective, environmentally friendly, user-friendly using small amounts of samples and simple or no preparation procedures (14). These advantages make it a promising alternative to traditional methods for determining drug concentrations across a wide range (15,16).
FTMIR spectroscopy, particularly in the ATR mode, is widely applied in quality control across industries such as pharmaceuticals, serving to identify and quantify active ingredients, excipients, and impurities (17).
In pharmaceutical sciences, this technique—whether using KBr pellets or ATR—is highly effective for both qualitative and quantitative analyses. Its simplicity, reliability, and lower cost compared to mass spectrometry (18–22) make it a preferred choice in industrial and research settings (23–25). However, no studies have yet employed FTMIR methods to determine low levels of organic impurities like NAs. This work thus aimed to qualitatively characterize and quantitatively establish the limit of quantification (LOQ) and detection (LOD) for NDBA, NDEA, NDMA, and NDIPA, using KBr-pellet and ATR-FTMIR approaches, followed by a comparative evaluation of the results from both methods.

Materials and methods

Chemicals

The NAs reference standard substances (99.0%) N-nitrosodimethylamine (NDMA), N-nitrosodiisopropylamine (NDIPA), and N-nitrosodibutylamine (NDBA) were purchased from Sigma-Aldrich (St. Louis, Missouri, USA) at 1 g mL^{-1}. N-nitrosodiethylamine (NDEA) was purchased from Toronto Research Chemicals (TRC) at 1 g mL^{-1} (Toronto, Ontario, Canada). Methanol HPLC (High Performance Liquid Chromatography) grade was obtained from J.T. BAKER®, 99.9%. KBr infrared grade, used in both tablets and dilutions for preliminary analysis by ATR, was purchased from Perkin-Elmer™ supplier (Waltham, Massachusetts, USA

Instrumentation

The NAs reference standard substances (99.0%) FTMIR spectra were obtained using a Perkin Elmer™ Frontier (Waltham, Massachusetts, EUA) with a KBr pellet or disk support system (traditional FTMIR technique). The beam entered the sample compartment, was transmitted through the sample, hit the detector, and formed spectra. The background spectrum was obtained by measuring the blank pellet containing KBr.
ATR-FTIR spectra were collected using a Perkin Elmer™ Frontier (Waltham, Massachusetts, EUA), FT-MIR Spectrometer equipped with an ATR sampling accessory. The background spectrum was obtained by measuring the clean ATR Zinc Selenide (ZnSe) crystal containing KBr only before each sample measurement. The ATR crystal plate surface was carefully cleaned with acetone after scanning each sample to remove any traces of the preceding sample.
FTMIR and ATR-FTMIR analysis involved 16 scans per replicate in the range of 4000–400 cm^{-1} and 4000–650 cm^{-1} with a resolution of 4 cm^{-1}, respectively. The bands values were analysed with the software Perkin Elmer™ Spectrum 10 version 4.2 and OriginPro® version 2018b. The same spectrometer was used for both FTMIR and ATR accessories.

Sample preparation

In this study, there were two stages. The first step was the experiment meant to find LOQ and LOD in methanol

using the ATR-FTMIR technique while the second step aimed to measure the LOD and LOQ in KBr using both FTMIR KBr-pellet and ATR-FTMIR methodologies. Initially, the KBr was dried at 105°C for 2 hours as a pre-treatment step. Each NA reference standard substance was individually mixed with KBr in different ratios in accordance to the literature (26).

LOQ and LOD in methanol by ATR-FTMIR

A preliminary evaluation was conducted using successive dilutions of the NDEA standard in methanol at ratios of 1:10, 1:20, 1:50, and 1:100, corresponding to 10%, 5%, 2.5%, and 1.0% (v/v), respectively.

LOQ and LOD by FTMIR KBr-pellet and ATR-FTMIR

The samples were evaluated individually using both KBr pellet and ATR methodologies simultaneously. Specifically, 200 mg of KBr was weighed, and sufficient amounts of NDMA, NDEA, NDIPA and NDBA standards were added at ratios of 1:200000, 1:100000, 1:50000, 1:33300, and 1:20000, respectively corresponding to 0.0005%, 0.001%, 0.002%, 0.003%, and 0.005% (m/v). The sample was mixed thoroughly with ground KBr using a mortar and pestle. The mixtures were divided into two 100 mg aliquots: one set was prepared in successive dilution concentrations, then pressed into samples for 30 seconds at 10 MPa pressure using a tableting mold for measurement using the KBr pellet technique, while the other set was directly evaluated on the ATR device. The assessment of the samples was conducted individually, simultaneously, and in real-time. The purpose of this approach, using KBr was to mimic a drug substance (DS) contaminated with NAs and to measure the ability of the techniques (FTMIR and ATR-FTMIR) to qualitatively and quantitatively evaluate the presence of NAs in the sample.

Determination of LOD and LOQ

The LOD is the lowest concentration of an analyte that can be reliably distinguished or the lowest amount of analyte in a sample that can be detected from the background noise, but not necessarily quantified as an exact value. According to the S/N approach, LOD is defined as the analyte concentration at which the S/N ratio is at least 3:1 (S/N = 3). A S/N ratio of at least 3:1 is generally considered acceptable for estimating the LOD. LOQ is the lowest concentration of an analyte that can be quantified with acceptable precision and accuracy. Using the S/N approach, LOQ is defined as the analyte concentration at which the S/N ratio is at least 10:1 (S/N = 10). The LOD and LOQ signal-to-noise ratio (S/N) were determined by measuring the equipment impedance without a sample or blank. Determining the signal-to-noise (S/N) ratio involves comparing the measured signals from samples with known low concentrations of analyte to those obtained from noise (equipment impedance only), which account for background environmental radiation and by establishing the minimum concentration at which the analyte can be reliably quantified (27,28).

Results and Discussion

The ATR-FTMIR was employed as the tool for the quantitative assessment of NAs in methanol. Successive dilutions of N-nitrosodiethanolamine (NDEA) in methanol were prepared to experimentally determine the LOD and LOQ. For the qualitative evaluation of NAs in KBr, ATR-FTIR and traditional FTMIR KBr-pellet methods were employed. The NA standards (NDMA, NDEA, NDIPA, NDBA) were mixed with KBr and analysed using both techniques. In the quantitative assessment, ATR-FTIR and FTMIR KBr pellets methodologies were applied, with KBr as a medium, for the LOD and LOQ of the NA standards mixed with KBr at different concentration ratios. Using ATR-FTIR and FTMIR KBr-pellets as a tool in direct quantitative measurement to determine the LOD and LOQ of NA standards mixed with KBr at different concentration ratios. The NA-KBr mixtures were analysed by FTMIR KBr-pellets as well as by direct use of ATR method.

Quantitative approach between ATR-FTMIR in methanol

The initial experiments utilized the ATR-FTMIR technique to determine the LOD and LOQ for NDEA. A standard calibration curve for NDEA was established by preparing various concentrations ranging from 0.5% to 10% (v/v), with the NDEA diluted in methanol. Figure 2 illustrates the intensity of absorption peaks for NDEA at concentrations of 1%, 2%, 3%, 5%, and 10% (v/v), as assessed by ATR-FTMIR in the wavenumber range of 4000–650 cm^{-1}. In preliminary tests, the analytical signal obtained through ATR-FTMIR for NDEA dissolved in methanol visually disappeared at concentrations below 2.5%, making it indistinguishable from the S/N ratio. However, the limits of detection (LOD) and quantification (LOQ) calculated approximately— $2.77x10^{-3}$ and $9.22x10^{-3}$% respectively—are significantly higher than the levels recommended by current regulations, $1.25x10^{-5}$% for losartan concerning NDEA, NDIPA, NDBA and $9.6x10^{-5}$% to NDMA respectively, for losartan (100 mg) maximum daily dose (MDD). These results show that the LOD and LOQ determined for NDEA are substantially greater than the values currently recommended, suggesting limited sensitivity of the technique for this specific analyte under the conditions tested.

Despite these changes, it was confirmed that the linear stretching and angular deformation of the nitrosamine (NA) functional groups were unaffected, and the important vibrational features of NA were still clearly observed. It has been demonstrated that the absorbance of FTMIR KBr-pellets and ATR-FTIR has a nonlinear correlation with concentration, not being in accordance to Lambert-Beer's law.

Quantitative approach between ATR-FTMIR and FTMIR measurements

The absorption peak intensities varied significantly when the samples were mixed with KBr at different proportions, indicating that the accuracy of the experimental results was strongly influenced by the sample preparation procedure (29). To ensure high selectivity, the spectral region between 1346 and 1265 cm^{-1}, corresponding to broad and intense bands typically attributed to N=O stretching vibrations, was selected for quantitative analysis. Figure 3 presents the spectra of NDBA, NDEA, NDMA, and NDIPA dissolved in KBr at concentrations of 0.005%, 0.003%, 0.002%, 0.001%, and 0.0005% (w/v), represented by black, red, blue, green, and purple lines, respectively, as obtained using the FTMIR KBr pellet and ATR-FTMIR techniques.

The dilution of samples in the range 0.0005-0.005% (m/v) in KBr ensured that absorbance bands were in the nonlinear range of Lambert–Beer's law. The preparation of KBr-pellets relied on a standardized procedure, for example, constant sample/KBr weight ratio, grinding time, pressure, and pellet weight to enhance reproducibility.

The sensitivity of FTMIR in KBr-pellets was significantly enhanced by the expanded range of optical throughput, while the sensitivity of ATR-FTMIR varied based on the wavenumber. In ATR-FTMIR the absorption peaks become stronger at long wavelengths but weaker at short wavelengths, resulting in the decreased sensitivity and weaker intensity of the functional group peaks owing to the greater penetration depth. This was the most important experimental difference between ATR-FTMIR and FTMIR, and it also explains because ATR spectroscopy has decreased sensitivity in the short wavelength region. Therefore, suitable infrared procedures should be used for samples with different requirements. The ATR-FTIR methodology using KBr as a diluent displayed greater sensitivity for all Nas compared to the FTMIR KBr-pellet method, primarily due to its superior S/N ratio. The results of the four Nas, and LOQ and LOD obtained approximately which were compared individually using both the FTMIR KBr-pellet and ATR-FTIR methods, are presented in Table 1.

Qualitative approach between ATR-FTMIR and FTMIR measurements

The MIR spectra of standard NDBA, NDEA, NDMA and NDIPA were obtained using the FTMIR KBr-pellets technique in the wavenumber range of 4000–400 cm^{-1} and ATR-MIR spectra were obtained in the wavenumber range of 4000–650 cm^{-1}. The theoretical four predicted stretching vibrations of relevance can be assigned as group frequencies: N=O, N-N, and C-N (symmetrical and asymmetrical). However, the spectra of NAs studied exhibits only three strong peaks in the region 1600-1000 cm^{-1} (30).

This range can be regarded as the fingerprint region for NAs (region 1), owing to the specific stretching vibrations of these compounds within this range (4000-400 cm^{-1}). Nonetheless, other generic stretching vibrations or bending can also be associated with the frequencies of aliphatic or alkyl groups: CH_3 and $-CH_2$ linked to the nitroso group (region 2).

The qualitative spectra were shown in Figure. 4, FTMIR KBr-pellet spectra (a) and ATR-FTMIR (b) methodologies, respectively in KBr of the NAs NDBA (red), NDEA (orange), NDMA (cyan) and NDIPA (blue) concentred at 5% (m/v).

The FTMIR and ATR-FTMIR shown highest intensity bands (region 1) at 1435 cm^{-1} bands of N=O stretching vibration of N-NO group, and the absorption of N-N vibration at 1022 cm^{-1}, respectively, while vibration of C-N gave two bands at 1304 and 1178cm^{-1} The strong band at 1460cm^{-1} assigned to dimeric linear stretching (νN=O) and the strong bands at 1313 and 1292cm^{-1} as dimeric linear stretching (νC-N) frequencies (31). along with 1460cm^{-1} related to bending vibrations of CH_2 and CH_3 aliphatic groups and 989cm^{-1} were assigned to $-CH_2$ rock and $-CH_2$ wagging and rocking. Low intensity bands at 2977cm^{-1} and 2911cm^{-1} correspond to $-CH_3$ stretching, while the band at 1470 cm^{-1} assigned to the monomeric linear stretching (νN=O), overlapped for the dimer bands. Finally, peaks at 1298cm^{-1}, 1105cm^{-1}, were designated to angular deformation (δCH_2) $-CH_2$ scissors, $-CH_2$ symmetric stretching vibrations, respectively (Table 2) (32).

The FTMIR KBr-pellet spectra absorption allows for selecting the fingerprint region, which shows clear variations in the detection of the added NDBA (red), NDEA (orange), NDMA (cyan) and NDIPA (blue) respectively.

Comparing the spectra, the intensities of peaks in the FTMIR KBr-pellet spectra were stronger than those in the ATR-FTMIR spectra. As short-wavelength light cannot penetrate the sample, the strength of the absorption peak in the ATR-FTMIR spectra decreases with decreasing wavelength, resulting in a significant reduction in absorption peak intensity in both functional group region 1 and region 2 (33). More detailed studies showed absorption peaks in the 3000–2900 cm^{-1} range (32) and bands at lower wavelengths (754 and 688 cm^{-1}) corresponded to C—H out-of-plane bonds for generic aliphatic bands both (region 1)(34), as well as linear stretching of N=O. According to Williams and Yoshimura et al. (31,34) the band at 1460 cm^{-1} could be assigned to this vibration mode.

Two sharp peaks at 1265 and 1227 cm^{-1} were typical of the N=O stretching mode, whereas a stronger signal at 907 cm^{-1} was assigned to the skeletal vibrations of the ONNO group (dimer). Linear stretching of N—N (νN-N) was observed between 1160 and 1050 cm^{-1}, and C—N was noted at 1550 and 1100 cm^{-1}. More specifically, two medium bands at 1335 and 1315 cm^{-1} were attributed to N—N and C—N stretching vibrations, respectively (35).

Additionally, the features between 1160 and 1050 cm^{-1} were the C—N in-plane bending modes (34), typical of the NAs "fingerprint". The presence of nitrogen functional groups was the key to NAs analysis, which is more evident in FTMIR spectra KBr technique.

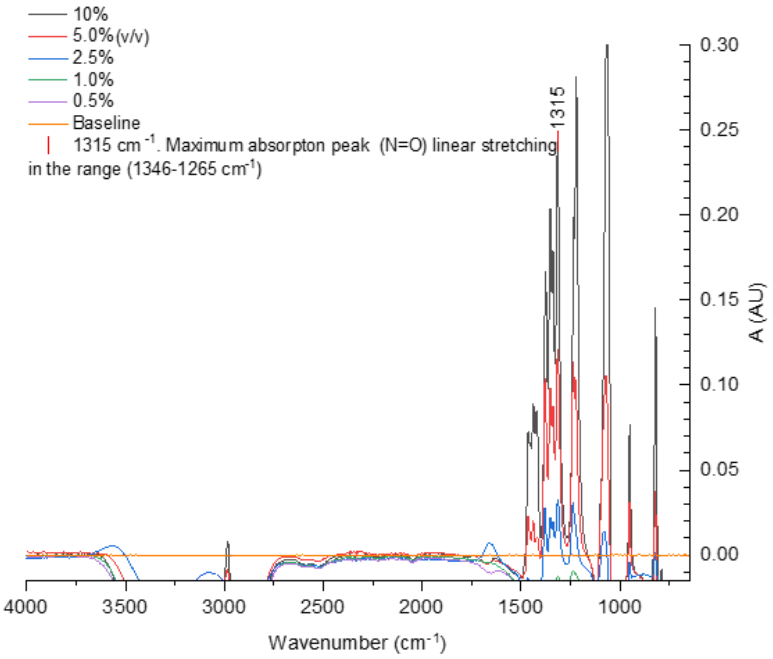

Figure 2 - Spectrum of NDEA standard dissolved in methanol at different concentrations 10%, 5%, 3%, 2%, and 1% (v/v) black, red, blue, green and purple respectively obtained by ATR-FTMIR intensity of absorption peaks between 4000–650 cm^{-1}

Table 1. Comparison of the LOD and LOQ achieved using both the FTMIR KBr-pellet and ATR-FTIR methods for NDBA, NDEA, NDIPA, and NDMA.

Methods	**NAs**	**LOD (%)**	**LOQ (%)**	**Limits to 100 mg of losartan (%)**
ATR-FTMIR (KBr)	NDBA	$1.44x10^{-3}$	$4.81x10^{-3}$	$1.2x10^{-5}$
	NDEA	$8.78x10^{-4}$	$2.93\ x10^{-3}$	$1.2\ x10^{-5}$
	NDIPA	$1.11x10^{-3}$	$3.70\ x10^{-3}$	$1.2\ x10^{-5}$
	NDMA	$4.94\ x10^{-4}$	$1.65\ x10^{-3}$	$9.6\ x10^{-5}$
FTMIR-KBr pellets	NDBA	$5.52x10^{-6}$	$1,83x10^{-5}$	$1.2\ x10^{-5}$
	NDEA	$2.01x10^{-5}$	$6.69x10^{-5}$	$1.2\ x10^{-5}$
	NDIPA	$1.07x10^{-5}$	$3.58\ x10^{-5}$	$1.2\ x10^{-5}$
	NDMA	$3.05x10^{-5}$	$1.02x10^{-4}$	$9.6\ x10^{-5}$

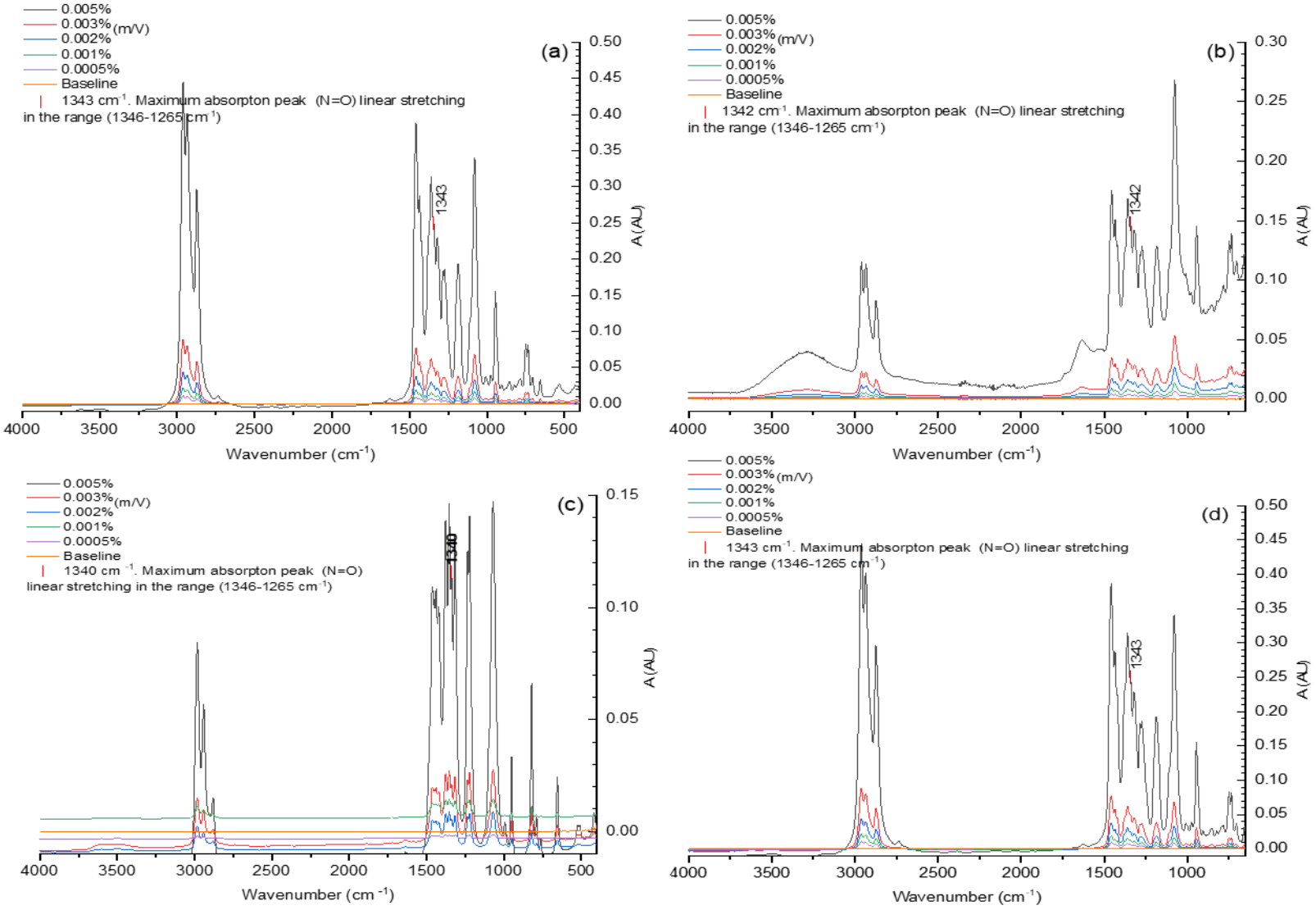
(a)
0.005%
0.003% (m/V)
0.002%
0.001%
0.0005%
Baseline
1343 cm-1. Maximum absorpton peak (N=O) linear stretching in the range (1346-1265 cm-1)
1343
A (AU)
Wavenumber (cm-1)
(b)
1342 cm-1. Maximum absorpton peak (N=O) linear stretching in the range (1346-1265 cm-1)
1342
(c)
1340 cm -1. Maximum absorpton peak (N=O) linear stretching in the range (1346-1265 cm-1)
1340
(d)
1343 cm-1. Maximum absorpton peak (N=O) linear stretching in the range (1346-1265 cm-1)
1343

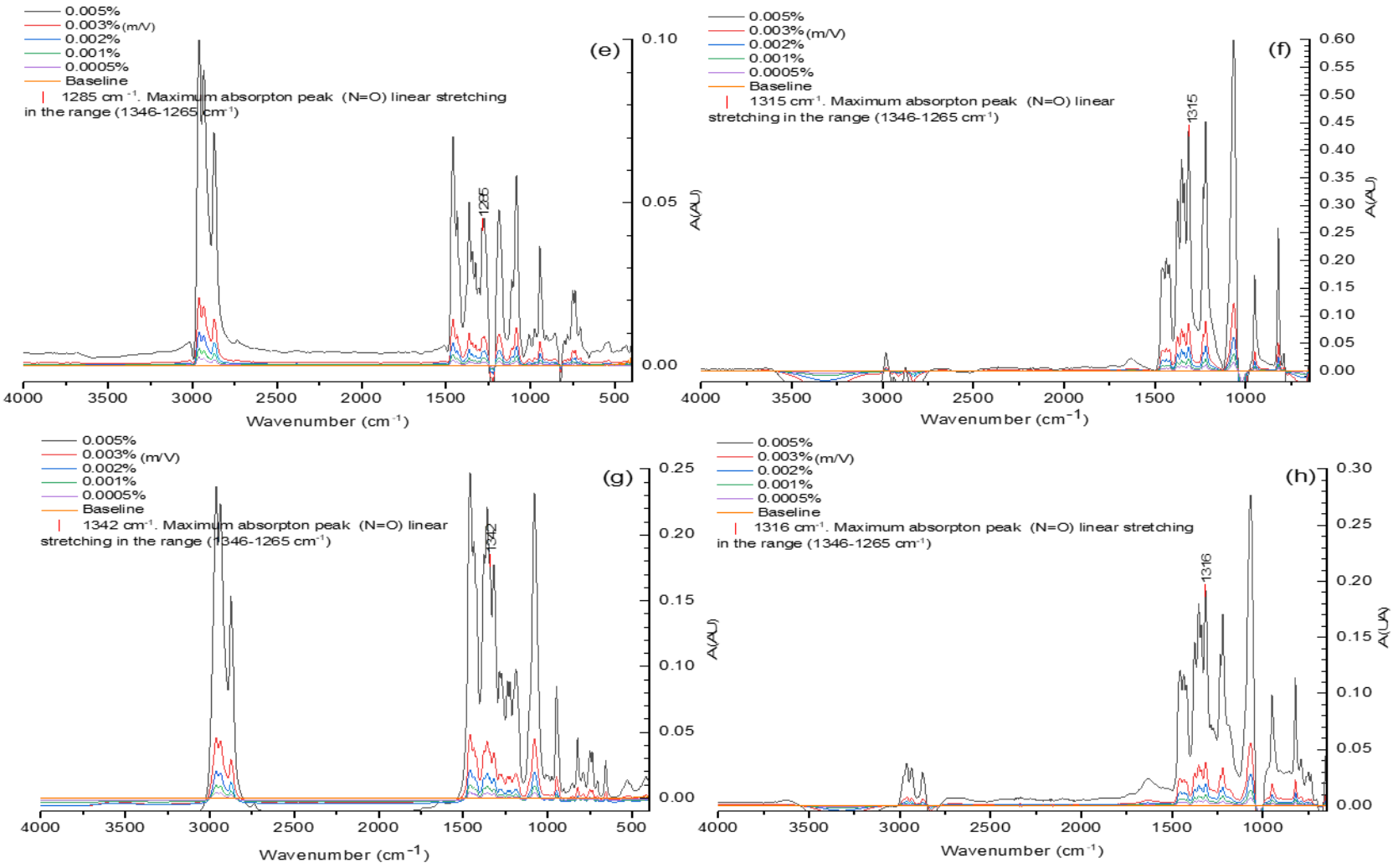

Figure 3 – Quantitative spectra of NDBA by FTMIR KBr pellet (a) and ATR-FTMIR (b); of NDEA by FTMIR KBr pellet (c) and ATR-FTMIR (d); of NDMA by FTMIR KBr pellet (e) and ATR-FTMIR (f); of NDIPA by FTMIR KBr pellet (g) and ATR-FTMIR (h) dissolved in KBr at different concentrations 0.005%, 0.003%, 0.002%, 0.001% and 0.0005% (m/v), black, red, blue, green and purple respectively.

Table 2. The FTMIR spectral region demonstrates the range, functional groups, and vibrations of NAs common bands observed in KBr pellets and ATR methods.

Bending/ Vibration	**Region (cm^{-1})**	**Observation**	**References**
	Region 1 – NAs fingerprint		
N=O($\nu_{N=O}$)	1486-1408; 1488	Linear stretching attached to monomer N=O unbound	(36,37)
	1346-1265; 1321-1292	Wide and strong bands typically related to NAs	(36)
	1317; 1460	Bands assigned to dimer linear stretching N = O	(31,37)
N—N (ν_{N-N}):	1106-1052	Linear stretching N—N	(36)
	1093-1047	Linear stretching N—N	(37)
	1160-1040	Linear stretching N—N	(38)
C—N (ν_{C-N})	1525; 1110	Bands moderate and strong intensities linear stretching C—N = O (1506 cm^{-1}) and C—N. linear stretching (1108 cm^{-1}) respectively	(39)
	1513	Linear stretching C—N = O	(37)
	1550-1430	Linear stretching C—N	(38)
	1313; 1292	Bands assigned to dimer C—N	(31)
	1100	Linear stretching C—N.	(36)
	Region 2 – Alkyl goup substituents		
—CH_3(ν_{C-H})	2977; 2911	Primary CH_3 stretching	(32)
CH_2—CH_3	1460	Bending vibrations of CH_2 and CH_3 aliphatic groups	
CH_2 (δC-H)	1298, 1105	Angular deformation (δCH_2) −CH_2 scissors, −CH_2 symmetric stretching vibrations	
CH_2 and CH_3	989	Assigned to −CH_2 rock and −CH_2 wagging and rocking	

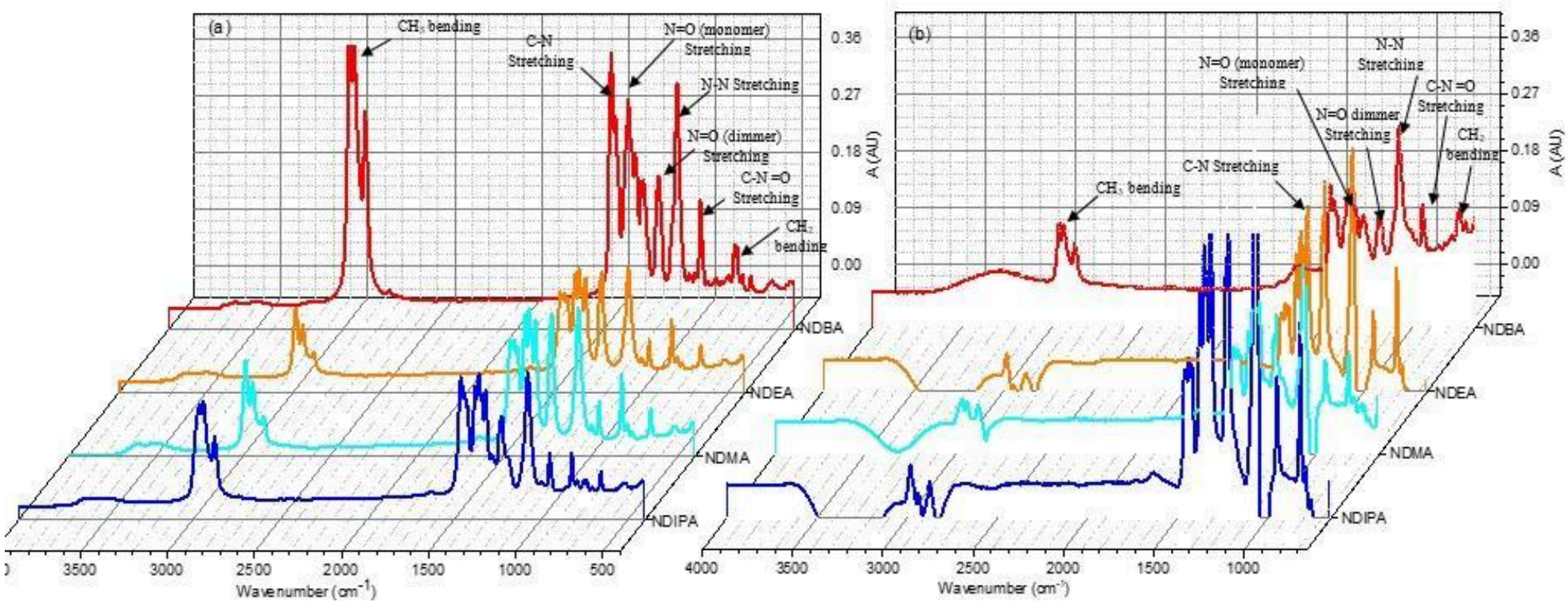

Figure 4. Displays the quantitative spectra obtained via the FTMIR KBr pellet (a) and ATR-FTMIR (b) methods for NDBA (red), NDEA (orange), NDMA (cyan), and NDIPA (blue), all concentrated at 5%, along with related observations.

Comparison of FTMIR KBr-pellet and ATR-FT-IR techniques

Similarly, to preliminary tests, the study was extended to prepare different concentrations ranging from 0.0005% to 0.005% (m/v), where NDBA, NDEA, NDIPA and NDMA was diluted with dried KBr and ground in agate mortar for 10 seconds to obtain a homogeneous sample. This was done to assess the LOD and LOQ of the ATR-FTMIR technique alongside the FTMIR KBr-pellets technique simultaneously. The sensitivity is notably influenced by the diluents, methanol, and KBr, possibly due to methanol interference in the previous ATR-FTIR analysis. However, it was possible to determine LOQ and LOD. According to Table 2, the FTMIR KBr-pellets method demonstrated lower LOD and LOQ than the ATR-FTMIR method, indicating greater sensitivity. The sensitivity is notably affected by the diluents, methanol, and KBr, possibly due to methanol interference and KBr is inactive in IR spectroscopy in the previous FTMIR KBr-pellets and ATR-FTMIR methodologies**.** In this study, FTMIR and ATR-FTMIR were employed to assess the effect of solvents with different physical and chemical properties, specifically methanol and KBr. Hypochromic and bathochromic shifts were observed, affecting the absorption intensity, frequency (wavenumber), and band position, as identified by Bellamy (40).

More detailed studies showed absorption peaks in the 3000–2900 cm^{-1} range (32) and bands at lower wavelengths (754 and 688 cm^{-1}) corresponded to C—H out-of-plane bonds for generic aliphatic bands both (34) (region 1), as well as linear stretching of N=O (νN=O). According to Williams and Yoshimura et al. (31,34), the band at 1460 cm^{-1} could be assigned to this vibration mode. Two sharp peaks at 1265 and 1227 cm^{-1} were typical of the N=O stretching mode, whereas a stronger signal at 907 cm^{-1} was assigned to the skeletal vibrations of the ONNO group (dimer). Linear stretching of N—N (νN-N) was observed between 1160 and 1050 cm^{-1}, and C—N was noted at 1550 and 1100 cm^{-1}. More specifically, two medium bands at 1335 and 1315 cm^{-1} were attributed to N—N and C—N stretching vibrations, respectively (35). Additionally, the features between 1160 and 1050 cm^{-1} were the C—N in-plane bending modes (34) typical of the NAs "fingerprint" region (region 2). The presence of nitrogen functional groups was the key to NAs analysis, which is more evident in FTMIR KBr-pellet spectra.

Based on the comparative analysis of FTMIR KBr-pellet and ATR-FTMIR for NAs, the differences in the crucial absorption intensity of the peaks for NDBA, NDEA, NDMA and NDIPA, in both region 1, and region 2 between the two infrared methods they had higher peak intensities in the FTMIR KBr-pellet were summarized in detail in Table 1. However, there were no significant frequency shifts, and the positions of functional group peaks obtained from ATR-FTMIR were consistent with those obtained from FTMIR.

The FTMIR KBr-pellet analysis needs sample preparation with many interfering factors and stringent KBr drying requirements, whereas ATR-FTMIR did not require a specific sample shape or water content and was non-destructive. Compared to FTMIR KBr-pellet, moisture absorption had a greater impact on the analysis of samples with OH groups in ATR-FTMIR. Moisture absorption interfered with the analysis of samples with OH groups more in the ATR-FTMIR than FTMIR KBr-pellet (41).

The peak at 3442 cm^{-1}, which is associated with O–H stretching, was observed in the FTMIR KBr-pellet spectra for all NAs. In the ATR-FTMIR spectra, this peak appeared as "blank absorption" for NDEA, NDMA, and NDIPA, and as positive absorption for NDBA. This shift in the spectral band has been suggested to be due to moisture absorption when the sample was ground with KBr (42) or standard containing methanol as diluent.

The peak intensities of functional groups in ATR-FTMIR spectra were significantly lower than in FTMIR KBr-pellet spectra. This was due to the short wavelength of reflection not penetrating deeply into the sample (42). Therefore, both FTMIR KBr-pellet and ATR-FTMIR were suitable for monitoring the functional groups of NAs and quantifying them in amounts LOD and LOD higher than those recommended by regulatory bodies. Even though the analysis of the high-quality standard substances was complicated by infrared techniques both, the monitoring results of functional groups obtained by the two infrared methodologies were significantly different. However, the peak sharpness in the spectra obtained by the two methodologies were essentially similar.

The effect of different solvents on the positioning of infrared spectrum bands have been have extensively investigated. The findings reveal that the frequency of X=O bonds shifts to lower values when transitioning from non-polar to polar solvents. While the frequency of X=O linkages changes consistently with a reference standard, X-H groups exhibit a different response to solvent variations. Tracking vibration frequencies across various solvents aids in the accurate assignment of these vibrations. Specifically, the X=O bond experiences a frequency reduction in polar solvents due to enhanced polar resonance. This insight improves the understanding of molecular structures as influenced by solvent types (40,43,44).

In this study, FTMIR and ATR-FTMIR were employed to assess the effect of solvents with different physical and chemical properties, specifically methanol and KBr (45). Hypochromic and bathochromic shifts were observed, affecting the absorption intensity, frequency (wavenumber), and band position, as identified by Bellamy. Despite these changes, it was confirmed that the linear stretching and angular deformation of the NA functional groups were unaffected, and the important vibrational features of NA were still clearly observed.

Conclusions

The qualitative comparison between the FTMIR KBr-pellet and ATR-FTMIR methodologies enabled the identification of characteristic spectral features of four nitrosamines (NDMA, NDEA, NDIPA, and NDBA) relevant to Quality Assurance/Quality Control (QA/QC) of nitrosamine impurities. Both techniques exhibited similar absorption bands, particularly within the fingerprint region, although slight differences in spectral profiles were observed. The evaluation of analytical sensitivity revealed that only the FTMIR KBr-pellet method achieved limits of detection (LOD) within the regulatory requirements for the qualitative detection of NDBA and NDIPA. In contrast, the LOD obtained for NDEA and NDMA, as well as all LOD values generated by the ATR-FTMIR methodology, exceeded the recommended regulatory limits. Furthermore, none of the limits of quantification (LOQ) obtained by either technique met the regulatory requirements for any of the evaluated nitrosamines. In addition, both techniques showed limitations related to reproducibility and repeatability, likely associated with the volatility and physicochemical properties of the nitrosamines. A nonlinear relationship between concentration and spectral response was also observed, indicating deviations from the Beer–Lambert law within the concentration ranges investigated. Based on these findings, the results do not support the use of FTMIR KBr-pellet or ATR-FTMIR as standalone methods for the reliable qualitative and quantitative determination of all evaluated nitrosamines at the concentration levels required by current regulatory guidelines. Consequently, more sensitive analytical techniques, particularly mass spectrometry-based methods, remain necessary for the accurate detection and quantification of these impurities in pharmaceutical products.

Author contributions

P.R.R.M. - methodology, data curation and original draft writing. E.L.G.D. - data collection, validation, and supervision. C.S.P. writing – review and editing. A.S.L.M. - conceptualization, supervision, writing – review and editing.

Acknowledgments

The authors are grateful to National Council for Scientific and Technological Development (CNPq) for financial support. Additionally, the authors wish to thank to Federal University of Pampa Foundation (Campus Uruguaiana. Brazil). (Campus Uruguaiana, Brazil) and Pharmacy of Faculty (FacFar), Federal University of Rio Grande do Sul, Porto Alegre, Rio Grande do Sul, Brazil.

Conflict of interest

The authors confirm that there are no conflicts of interest.

Funding

This work was supported financially by CNPQ (process 302223/2025-8).

References

1. Medicines Agency European (EMA). Sartan medicines: companies to review manufacturing processes to avoid presence of nitrosamine impurities [Internet]. 2018. Report. Available from: www.ema.europa.eu/contact.
2. European Medicines Agency (EMA). EMA reviewing medicines containing valsartan from Zhejiang Huahai following detection of an impurity [Internet]. 2018 [cited 2024 Sep 30]. Report. Available from: www.ema.europa.eu/en/documents/press-release/ema-reviewing-medicines-containing-valsartan-zhejiang-huahai-following-detection-impurity_en.pdf.
3. Barnes JM, Magee PN. Some toxic properties of dimethylnitrosamine. Br J Ind Med. 1954;11(3):167. doi:10.1136/oem.11.3.167
4. Magee PN, Barnes JM. The production of malignant primary hepatic tumours in the rat by feeding dimethylnitrosamine. Br J Cancer. 1956;10(1):114. doi:10.1038/bjc.1956.15.
5. International Agency for Research on Cancer (IARC). World Health Organization (WHO). Some N-Nitroso Compounds. In: Monographs on the Evaluation of the Carcinogenic Risk of Chemicals to Humans. France; 1978.
6. Bişgin AT. Cloud Point Extraction and Spectrophotometric Determination of Allura Red (E129) in Foodstuffs. Iğdır Üniversitesi Fen Bilimleri Enstitüsü Dergisi. 2018 Dec 30;8(4):239–46. doi:10.21597/jist.397479.
7. Borba A, Gómez-Zavaglia A. Infrared spectroscopy: an underexploited analytical tool for assessing physicochemical properties of food products and processing. Curr Opin Food Sci. 2023 Feb;49:100953. doi:10.1016/j.cofs.2022.100953.
8. Burger A, Koller KT. Polymorphism without IR-and Raman-spectroscopic differences: tiaprofenic acid, three modifications. Pharmazie, 54(5). 1999;54(5):365–8.

9. Sun Y, Liu N, Zhao L, Liu Q, Wang S, Sun G, et al. Attenuated total reflectance-flourier transformed infrared spectroscopy (ATR-FTIR) coupled with deep learning: A rapid method for geographical origin identification of sea cucumber Apostichopus japonicus. Microchemical Journal. 2024 Sep;204:111037. doi:10.1016/j.microc.2024.111037.
10. Calvo NL, Maggio RM, Kaufman TS. Chemometrics-assisted solid-state characterization of pharmaceutically relevant materials. Polymorphic substances. J Pharm Biomed Anal. 2018 Jan;147:518–37. doi:10.1016/j.jpba.2017.06.018.
11. Baker AW. Solid State Anomalies in Infrared Spectroscopy. J Phys Chem. 1957 Apr 1;61(4):450–8. doi:10.1021/j150550a016.
12. Kurrey R, Mahilang M, Kanti Deb M, Nirmalkar J, Shrivas K, Pervez S, et al. A direct DRS-FTIR probe for rapid detection and quantification of fluoroquinolone antibiotics in poultry egg-yolk. Food Chem. 2019 Jan;270:459–66. doi:10.1016/j.foodchem.2018.07.129.
13. Karoui R. Spectroscopic Technique: Mid-Infrared (MIR) and Fourier Transform Mid-Infrared (FT-MIR) Spectroscopies. In: Modern Techniques for Food Authentication. Elsevier; 2018. p. 23–50. doi:10.1016/B978-0-12-814264-6.00002-5
14. Roberts JJ, Power A, Chapman J, Chandra S, Cozzolino D. Vibrational Spectroscopy Methods for Agro-Food Product Analysis. In. 2018. p. 51–68. doi:10.1016/bs.coac.2018.03.002
15. Mayerhöfer TG, Popp J. Beer's Law – Why Absorbance Depends (Almost) Linearly on Concentration. ChemPhysChem. 2019 Feb 18;20(4):511–5. doi:10.1002/cphc.201801073
16. Manouchehri F, Izadmanesh Y, Aghaee E, Ghasemi JB. Experimental, computational and chemometrics studies of BSA-vitamin B6 interaction by UV–Vis, FT-IR, fluorescence spectroscopy, molecular dynamics simulation and hard-soft modeling methods. Bioorg Chem. 2016 Oct;68:124–36. doi:10.1016/j.bioorg.2016.07.014
17. Bunaciu AA, Aboul-Enein HY. Adulterated drug analysis using FTIR spectroscopy. Appl Spectrosc Rev. 2021 May 28;56(5):423–37. doi:10.1080/05704928.2020.1811717
18. Kogawa AC, Nunes Salgado HR. Spectrophotometry in Infrared Region: A New, Low Cost and Green Way to Analyze Tablets of Rifaximin. Curr Pharm Anal. 2018 Jan 23;14(2). doi:10.2174/1573412913666161213103657
19. Souza Lima JG, De Marco BA, Salgado HRN. Green analytical method for quantification of Secnidazole in tablets by Fourier-Transform Infrared Spectroscopy (FTIR). Drug Analytical Research. 2018 Dec 16;2(2):14–9. doi:10.22456/2527-2616.88545
20. Nascimento P.A., Kogawa A.C., Salgado H.R.N. A green and sustainable method by infrared for quantitative determination of sodium cephalothin. Austin J Anal Pharm Chem. 2019;6:1117–21.
21. Rechelo BS, Kogawa AC, Salgado HRN. Quantitative analysis of cefazolin sodium in lyophilized powder by infrared spectrophotometry: Green, low cost, fast and effective. Spectrochim Acta A Mol Biomol Spectrosc. 2019 Feb;208:157–61. doi:10.1016/j.saa.2018.09.058
22. Nascimento PA do, Kogawa AC, Salgado HRN. A New and Ecological Method to Quantify Vancomycin in Pharmaceutical Product by Infrared Spectrometry. Acta Chim Slov. 2021 Jun 15;68(2):313–9. doi:10.17344/acsi.2020.6107
23. Silverstein RM, Webster FX, Kiemle D. Spectrometric Identification of Organic Compounds. 7th ed. Rio de Janeiro: LTC; 2007.
24. Pavia DL, Lampman GM, Kriz GS, Vyvyan JA. Introduction to Spectroscopy. 4th ed. Cengage Learning; 2015.
25. Corrêa JCR, Salgado HRN. A platform for designing quantitative infrared spectrophotometric method for drugs and pharmaceuticals analysis: a rediscover for an ecological and safer technique in the routine quality control laboratories. World J Pharm Pharm Sci [Internet]. 2014 [cited 2025 Jan 16];3(6). Available from: http://hdl.handle.net/11449/133784.
26. Kogawa A, Salgado HRN. Quantitative analysis of pharmaceutical products by spectrophotometry in the infrared region: a practical review. Drug Analytical Research. 2022 Jan 15;6(2):3–7. doi:10.22456/2527-2616.127631
27. International Conference on Harmonisation (ICH). International Conference on Harmonisation of Technical Requirements for Registration of Pharmaceuticals for Human Use ICH Harmonised Tripartite Guideline Validation of Analytical Procedures: Text and Methodology Q2(R1). Geneva; 2005. Report.
28. United States Pharmacopeia 36 - National Formulary 31 (USP-NF). General Information: <1225> Validation of Compendial Procedures. Rockville; 2012. Report.
29. Rajandas H, Parimannan S, Sathasivam K, Ravichandran M, Su Yin L. A novel FTIR-ATR spectroscopy-based technique for the estimation of low-density polyethylene biodegradation. Polym Test. 2012 Dec;31(8):1094–9. doi:10.1016/j.polymertesting.2012.07.015.
30. Looney CE, Phillips WD, Reilly EL. Nuclear Magnetic Resonance and Infrared Study of Hindered Rotation in Nitrosamines. J Am Chem Soc. 1957 Dec 1;79(23):6136–42. doi:10.1021/ja01580a009
31. Williams RL, Pace RJ, Jeacocke GJ. Applications of solvent effects—I. Spectrochimica Acta. 1964 Feb;20(2):225–36. doi:10.1016/0371-1951(64)80012-6

32. Chesalov YA, Chernobay GB, Andrushkevich T V. FTIR study of the surface complexes of β-picoline, 3-pyridine-carbaldehyde and nicotinic acid on sulfated TiO2 (anatase). J Mol Catal A Chem. 2013 Jul;373:96–107. doi:10.1016/j.molcata.2013.03.007
33. Crawford CB, Quinn B. The contemporary history of plastics. In: Microplastic Pollutants. Elsevier; 2017. p. 19–37. doi:10.1016/B978-0-12-809406-8.00002-5.
34. Yoshimura T, Miyake C, Imoto S. Ultraviolet and Infrared Spectra of Cupferron and Neocupferron. Bull Chem Soc Jpn. 1972 May 1;45(5):1424–30. doi:10.1246/bcsj.45.1424.
35. Jones RN, Sandorfy C. The application of infrared and Raman spectrometry to the elucidation of molecular structure. In: Chemical applications of spectroscopy. 1956. p. 247–580.
36. Tarte P. Recherches spectroscopiques sur les composés nitrosés. Bulletin des Sociétés Chimiques Belges. 1954 Jan;63(9–10):525–41. doi:10.1002/bscb.19540630907
37. Haszeldine RN, Jander J. Studies in spectroscopy. Part VI. Ultra-violet and infra-red spectra of nitrosamines, nitrites, and related compounds. Journal of the Chemical Society (Resumed). 1954;691–5.
38. Wishok JS. Encyclopedia of Chemical Technology: Matches to N-Nitrosamines. In: Mark HF et al., editor. Vol. 15. New York: John Wiley and Sons; 1981.
39. Lüttke W. Spektroskopische Untersuchungen an Nitrosoverbindungen 1. Mitteilung: Die charakteristischen Infrarotbanden der monomeren Nitrosoverbindungen. Zeitschrift für Elektrochemie, Berichte der Bunsengesellschaft für physikalische Chemie. 1957 Mar 4;61(2):302–13. doi:10.1002/bbpc.19570610213
40. Bellamy LJ, Conduit CP, Pace RJ, Williams RL. Infra-red spectra and solvent effects. Part 5.—Solvent effects on X=O dipoles and on rotational isomers. Trans Faraday Soc. 1959;55(0):1677–83. doi:10.1039/TF9595501677
41. Wang J, Wang Y, Li X, Weng Y, Dong X, Zhao X. Comparison on the effectiveness of Fourier transform infrared (FT-IR) and attenuated total reflection Fourier transform infrared (ATR-FT-IR) in characterizing plastics biodegradation by insect larvae. Science of The Total Environment. 2022 Sep; 839:156289. doi:10.1016/j.scitotenv.2022.156289
42. Canham L. Handbook of Porous Silicon. Canham L, editor. Cham: Springer International Publishing; 2014. doi:10.1007/978-3-319-71381-6
43. Bellamy LJ, Williams RL. Infra-red spectra and solvent effects. Part 2.—Carbonyl absorptions. Trans Faraday Soc. 1959;55(0):14–8. doi:10.1039/TF9595500014
44. Bellamy LJ, Hallam HE, Williams RL. Infra-red spectra and solvent effects. Part 1.—X—H stretching frequencies. Trans Faraday Soc. 1958;54(0):1120–7. doi:10.1039/TF9585401120
45. Figueroa-Ariza LT, Paez-Sierra BA. Solvent-dependent spectral deconvolution of amino-substituted chalcones: UV–vis and FT-IR analysis supported by TD-DFT calculations. J Mol Struct. 2026 Feb;1351:144083. doi:10.1016/j.molstruc.2025.144083